

How merging droplets jump off a superhydrophobic surface: Measurements and model

Timothée Mouterde,^{1,2,*} Thanh-Vinh Nguyen,^{3,†} Hidetoshi Takahashi,^{4,‡} Christophe Clanet,^{1,2,§}
Isao Shimoyama,^{3,4} and David Quéré^{1,2}

¹*Physique et Mécanique des Milieux Hétérogènes, UMR 7636 du CNRS, ESPCI, 75005 Paris, France*

²*Laboratoire d'Hydrodynamique de l'X, UMR 7646 du CNRS, École Polytechnique, 91128 Palaiseau, France*

³*Information and Robot Technology Research Initiative, The University of Tokyo, 7-3-1 Hongo, Bunkyo-ku, Tokyo, Japan*

⁴*Department of Mechano-Informatics, Graduate School of Information Science and Technology, The University of Tokyo, 7-3-1 Hongo, Bunkyo-ku, Tokyo, Japan*

(Received 6 June 2017; published 16 November 2017)

We investigate how drops merging on a nonwetable surface jump off this surface, for both symmetric and asymmetric coalescences. For this purpose, we design and build a microelectromechanical system sensor able to quantify forces down to the micro-Newton scale at a high acquisition rate (200 kHz). Using this device, we perform direct force measurements of self-propelled droplets coupled to high-speed imaging. Experimental data show that the total momentum of the drop after coalescence mainly depends on the size of the smaller drop. Exploiting this finding, we quantitatively predict the takeoff speed of jumping drop pairs and show how to correct the usual argument based on energy conservation.

DOI: [10.1103/PhysRevFluids.2.112001](https://doi.org/10.1103/PhysRevFluids.2.112001)

A water droplet deposited on micrometric hydrophobic features adopts a quasispherical shape, which makes it highly mobile [1]: Owing to the small amount of contact between the solid and liquid, drops somehow behave as hovercrafts. Logically, mobility vanishes when humidity condenses within the microtextures, which sticks water to its substrate [2–4]. However, even in such challenging conditions, a low adhesion can be maintained if the roughness is scaled down to typically 100 nm, that is, smaller than the average distance between two condensation nuclei [5–12]. On such tiny features, growing condensing drops at the scale of 10–100 μm or even smaller [11,12] can be ejected when coalescing with their neighbors, as first reported by Boreyko *et al.* [7]. Assuming a fully efficient transfer from surface energy (of order γR^2 , with γ the liquid surface tension and R the drop size) in kinetic energy (scaling as $\rho R^3 U^2$, with ρ the liquid density and U the takeoff velocity), we get a characteristic takeoff velocity $U^* = (\gamma/\rho R)^{1/2}$. This law has been tested by looking at the departure speed of pairs of drops coalescing either in a Leidenfrost situation [13], or on superhydrophobic surfaces [7]. In both cases, the scaling in $R^{-1/2}$ is obeyed, provided the drops are large enough to neglect the adhesion of water with the substrate. However, studies pointed out that the takeoff velocity is about five times smaller than predicted by energy conservation [7,14–16], which might arise from strong oscillations generated by coalescence [17]. Here, we try to understand these paradoxical observations (correct scaling law, wrong order of magnitude) by looking at the balance of forces during merging and departure.

Our experiment consists of simultaneously filming drops coalescing on a superhydrophobic material, and monitoring the force exerted on the substrate [Fig. 1(a)]. For the latter purpose, we

*timothee.mouterde@polytechnique.org

†vinh@leopard.t.u-tokyo.ac.jp

‡takahashi@leopard.t.u-tokyo.ac.jp

§clanet@ladhyx.polytechnique.fr

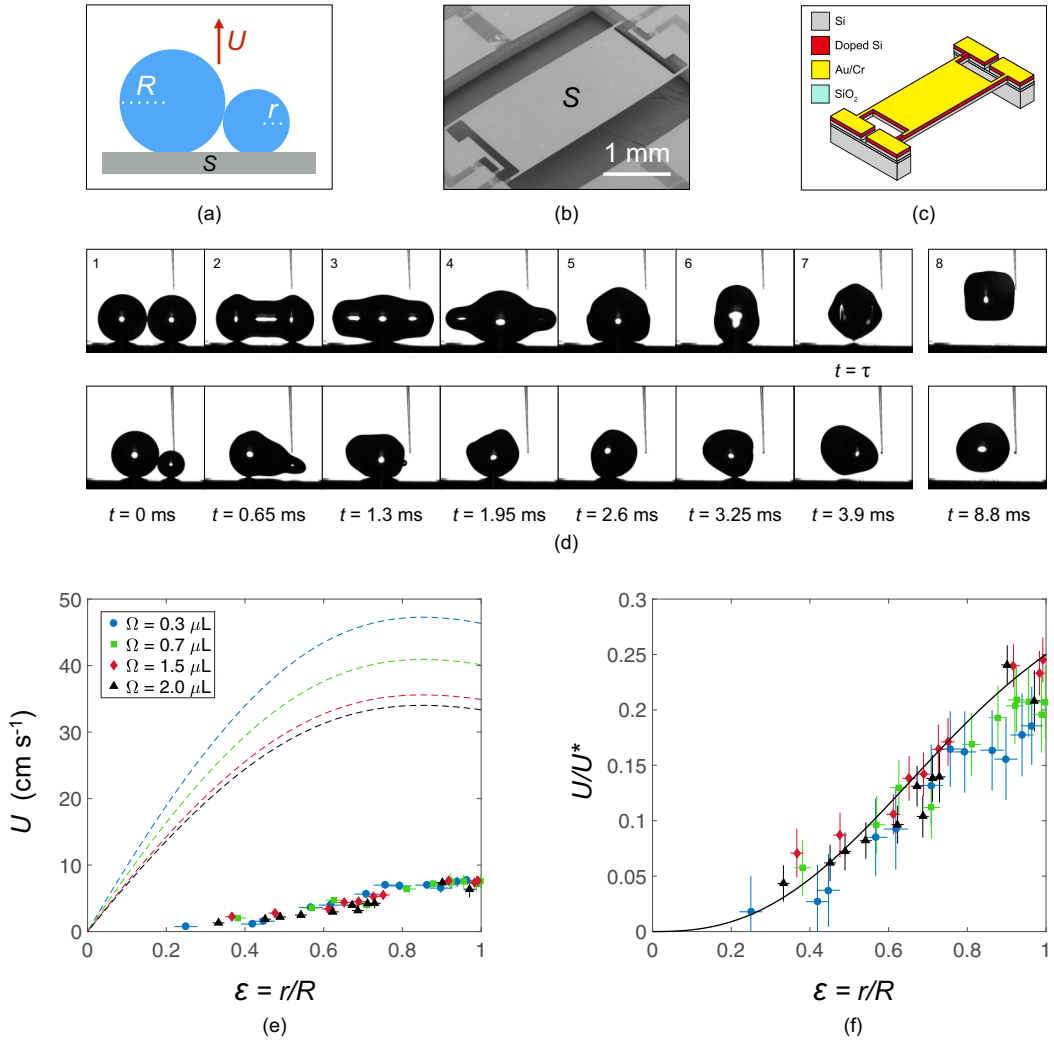
TIMOTHÉE MOUTERDE *et al.*


FIG. 1. (a) Sketch of an asymmetric coalescence between droplets with respective radius R and r ; the resulting drop jumps at a velocity U . (b) Scanning electron microscopy viewgraph of the MEMS designed to measure the forces induced by drops merging on a superhydrophobic surface S . (c) Sketch of the MEMS showing the different layers. Gray, red, yellow, and light blue respectively represent silicon, doped silicon, Au/Cr layer, and SiO_2 layer. (d) High-speed imaging of (top) a symmetric coalescence ($R = 530 \mu\text{m}$) and (bottom) an asymmetric coalescence ($R = 530 \mu\text{m}$ and $r = 300 \mu\text{m}$, $\varepsilon = r/R = 0.57$). Snapshot 1 shows the beginning of the coalescence, and snapshot 7 corresponds to takeoff. Images are separated by 0.65 ms , except snapshot 8 shot at 8.8 ms , when the drop reaches its maximum height. (e) Velocity U of jumping drops as a function of the ratio $\varepsilon = r/R$. Colors indicate the volume Ω of the large drop. Colored dashed lines show the speed expected from energy conservation, Eq. (1). (f) Same data after normalizing U by $U^* = \sqrt{\gamma/\rho R}$, as a function of ε . The solid line shows Eq. (3) drawn without an adjustable parameter.

construct the microelectromechanical system (MEMS) sensor shown in Fig. 1(b), following the procedure described in Nguyen *et al.* [18]. It is fabricated from a silicon-on-insulator (SOI) wafer, where the top surface is a piezoresistive layer, with thickness $5/2/300 \mu\text{m}$ [19]. Cr and Au layers with respective thicknesses of 5 and 50 nm are deposited and patterned using deep reactive ion etching. Piezoresistors are made by a second patterning of the Au/Cr layers, the handle silicon layer

HOW MERGING DROPLETS JUMP OFF A ...

is etched, and the sensor is released after etching the buried oxide layer using hydrogen fluoride vapor [Fig. 1(c)]. The device can measure forces applied on a field of $1.5 \text{ mm} \times 3 \text{ mm}$, with a sensitivity of $1 \mu\text{N}$, a quantity significantly smaller than the weight of our drops (the smallest one with volume $\Omega = 0.3 \mu\text{L}$ having a weight of $3 \mu\text{N}$).

The surface of the sensor is rendered to be water repellent using hydrophobic silica nanobeads dispersed in isopropanol (Mirror Coat Zero; Soft99). After evaporation of the solvent, the surface is rough and hydrophobic, and water on this texture exhibits advancing and receding contact angles $\theta_a = 165^\circ \pm 2^\circ$ and $\theta_r = 162^\circ \pm 2^\circ$, respectively. This combination of high angle and low hysteresis makes the surface highly nonadhesive, a necessary condition for observing jumping drops. Such observations are made by imaging pairs of drops deposited on the sensor at 20 000 frames per second (high-speed video camera Photron Fastcam SA-X2). Droplets are submillimetric and dispensed from superhydrophobic glass microneedles. We successively inflate a “large” drop with radius $R = 530 \pm 20 \mu\text{m}$ and volume $\Omega = 0.62 \pm 0.06 \mu\text{L}$ and a second one with radius r until contact triggers coalescence. r is varied between $0.2R$ and R , and the asymmetry is quantified by a number $\varepsilon = r/R$ spanning from ~ 0.2 to 1.

Typical merging/jumping processes are shown in Fig. 1(d) for both symmetric ($R = r = 530 \mu\text{m}$) and asymmetric configurations ($R = 530 \mu\text{m}$ and $r = 300 \mu\text{m}$, $r/R \approx 0.57$). In both cases, water leaves the substrate around $\tau = 3.9 \pm 0.1 \text{ ms}$, and the final snapshots show the maximum heights reached by the jumping drops. We observe that symmetric merging leads to a higher jump, meaning a larger takeoff velocity U . U is extracted from the movies by an image analysis: We determine and follow the position of the drop barycenter as a function of time t . By differentiating this curve with respect to t , we deduce the drop velocity along the flight. The maximum of this quantity (observed at small time, typically during the first 10 ms) is the jumping velocity.

We report in Fig. 1(e) the velocity U as a function of $\varepsilon = r/R$ for $\Omega = 0.27, 0.65, 1.51, \text{ and } 2 \mu\text{L}$, and varying the size of the small drop in the interval $0.2 \leq \varepsilon \leq 1$. We observe that the jumping velocity monotonously increases with ε : Smaller drops will logically communicate less momentum to the large one, which results in a slower takeoff. In the same figure, dashed lines show the law expected from a full transfer of surface energy (gained in coalescence) into kinetic energy, that is,

$$U = U^* \sqrt{\frac{6[\varepsilon^2 + 1 - (\varepsilon^3 + 1)^{2/3}]}{(\varepsilon^3 + 1)}}. \quad (1)$$

This law largely overestimates the data, both at small ε (where it reduces to $U \approx U^* \sqrt{6\varepsilon}$, a linear variation in ε), and for symmetric merging ($\varepsilon = 1$), where the predicted velocity $U \approx 1.11U^*$ is about five times larger than observed, as already reported in the literature [7,14–16]. In addition, conservation of energy predicts a maximum departure velocity for $\varepsilon \approx 0.85$ [20], while data show a monotonic behavior, as clearly visible in the dimensionless representation of Fig. 1(f). Hence the failure of energy conservation, obvious for symmetric merging, is found to be even more visible for asymmetric coalescences. We try to understand what fixes the speed U , by looking at the forces and characteristic times involved in coalescence.

In order to get more information about jumping, we couple high-speed imaging at 20 kHz to measurements of the force at 200 kHz during coalescence. We report in Fig. 2(a) the force F exerted on the substrate (minus the weight of the drops), for the symmetric (black line) and asymmetric (red line) coalescences displayed in Fig. 1(d). The origin of time is taken at contact, when the drops are still at rest ($F = 0$), and F is measured until drop departure, at time τ . Much information can be extracted from this plot. (1) Around $t = 0.5 \text{ ms}$, F decreases by typically $10 \mu\text{N}$, that is, the weight of the drops. A pressure wave at the surface of water temporarily detaches it from the surface, so that we transiently have $F = -(M + m)g$, where M and m are the respective masses of the two drops. (2) Later, forces exhibit a large peak, which appears earlier for asymmetric merging. Peaks correspond to the end of the recoiling stage [frame 5 and frame 4 in Fig. 1(d)]. (3) The peak magnitude is $\sim 100 \mu\text{N}$ for the asymmetric case, and $\sim 200 \mu\text{N}$ for the symmetric one, much larger than the weight. (4) Just prior to departure ($t \leq \tau$), the force becomes negative again due to the

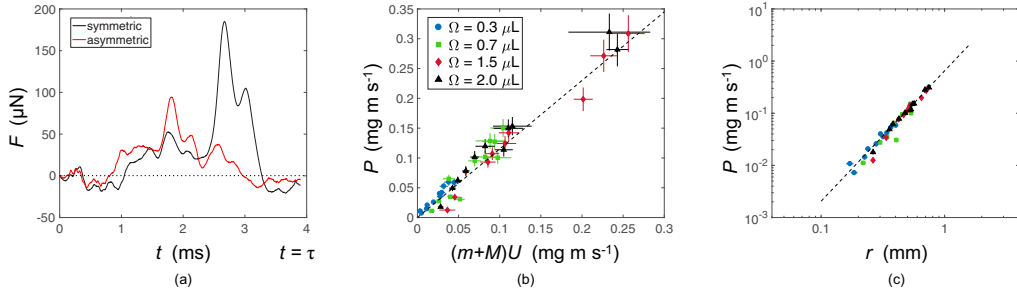
TIMOTHÉE MOUTERDE *et al.*


FIG. 2. (a) Force exerted by merging drops on their substrate, for the experiments shown in Fig. 1(d) (data sampled at 200 kHz). Black and red lines correspond respectively to symmetric and asymmetric coalescence. Time starts with contact ($t = 0$) and ends at takeoff ($t = \tau$). (b) Force integrated over the jumping time P as a function of the momentum $(M + m)U$ of the departing drop. The dashed line has a slope of 1.15. (c) P as a function of the small radius r . The dashed line shows a slope $5/2$.

upward motion that gradually detaches it from the substrate. (5) Integrating the force with respect to time provides the vertical momentum P . Performing this integration between $t = 0$ (contact) and $t = \tau$ (takeoff), we obtain

$$P = \int_0^\tau F dt = (M + m)U. \quad (2)$$

We gather our results in Fig. 2(b), where we plot the momentum $P = \int_0^\tau F dt$ deduced from the force measurement as a function of the quantity $(M + m)U$ deduced from jumping velocity measurements. Equation (2) is verified, as underlined by a dashed line of slope 1.15 (close to unity) in Fig. 2(b). Since momentum is generated by the motion of the small drop towards the large one, we also plot P as a function of r in Fig. 2(c). P is found to increase rapidly with r , and the log/log scales reveal a scaling law of exponent 2.5 ± 0.1 (dashed line). Remarkably, data obtained with different volumes Ω [color code defined in Fig. 2(b)] all collapse on the same curve.

As the small drop seems to play a key role in the jumping momentum, we focus on its dynamics [Fig. 3(a)]. We first consider the retraction time τ_r needed for the edge of the drop to travel by a radius r after contact, as shown in Fig. 3(b). The time τ_r , plotted as a function of r in Fig. 3(c), is observed to be independent of Ω and to vary as $r^{3/2}$ (dashed line), which expresses the classical balance between capillary force γr and inertia $\rho r^3(r/\tau_r^2)$. The resulting scaling law, $\tau_r \sim \sqrt{\rho r^3/\gamma}$, is represented in Fig. 3(c) with a coefficient 2 to fit the data.

We finally split up the coalescence process sketched in Fig. 3(a) into three steps. (i) When drops merge, surface tension generates a flow along the (roughly horizontal) axis of symmetry of the pair of drops. The fastest motion (or shortest time scale) is that of the small drop. It carries a momentum $p = mv$, where $v \approx r/\tau_r$ is the velocity of the drop edge. Hence a momentum $p \approx (2\pi/3)\sqrt{\rho\gamma r^5}$ [red arrow in Fig. 3(a)] that does not generate any pressure (yet) on the plate. (ii) During that time, the large drop opposes an equivalent momentum, and the incompressible fluid is deviated from a central stagnation point. Denoting η as the liquid viscosity, the Reynolds number is $\rho r^2/\eta\tau_r$, on the order of 100. Since viscous dissipation can be neglected, the maximum momentum deviated vertically from each drop is equal to the horizontal momentum mv , which eventually generates takeoff (iii).

This scenario can be tested. In Fig. 3(d), we plot P , the integral of the force over the jumping time, as a function of the momentum of the small drop, $mv \approx (2\pi/3)\sqrt{\rho\gamma r^5}$. As seen in Fig. 3(d), this curve is similar to the one in Fig. 2(b): The integral of the force compares to mv (the dashed line shows $y = 1.15x$), in agreement with the assumption that the small drop momentum is redirected to the substrate. Hence the momentum conservation can be written $(M + m)U = mv$, which yields

HOW MERGING DROPLETS JUMP OFF A ...

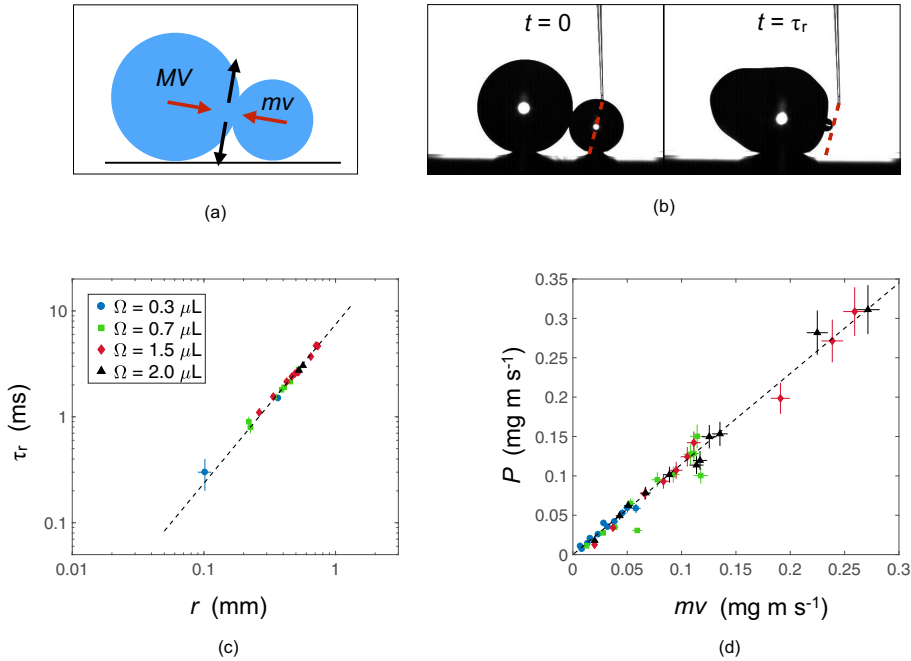


FIG. 3. (a) Schematic describing the transfer of quasihorizontal momentum of the small drop into quasivertical momentum. (b) Snapshots 1 and 3 of the asymmetric coalescence in Fig. 1(d) illustrating the retraction time τ_r , defined as the time needed for the edge of the small drop to move by its own radius. In this example, we have $\tau_r \approx 1.3$ ms. (c) Retraction time τ_r as a function of r . The black dashed line shows $\tau_r = 2\sqrt{\rho r^3/\gamma}$. (d) Force integrated over the jumping time as a function of the measured momentum $mv = mr/\tau_r$ of the small drop. The dashed line has a slope 1.15.

the takeoff velocity U ,

$$U = \frac{1}{2}U^* \frac{\varepsilon^{5/2}}{\varepsilon^3 + 1}. \quad (3)$$

Equation (3) is drawn with a solid line in Fig. 1(f), where it is found to nicely describe the data, without any adjustable parameter. First, all data collapse on the same curve, that monotonously increases as coalescence is more and more symmetric. Second, asymmetric coalescences ($\varepsilon \ll 1$) are captured by Eq. (3) that writes in this limit $U \approx \frac{1}{2}U^*\varepsilon^{5/2}$, a function that decreases very rapidly as the coalescence becomes asymmetric. Third, U increases linearly with ε as approaching symmetric coalescences, where Eq. (3) becomes $U \approx U^*\varepsilon/4$. For $\varepsilon \approx 1$, we observe $U \approx 0.2U^*$, close to the value $U = U^*/4$ predicted by Eq. (3), and far from the velocity $U = (3[2 - 2^{2/3}])^{1/2}U^* \approx 1.11U^*$, expected from energy conservation Eq. (1). Our model slightly overestimates the speed of symmetric jumps by $\sim 15\%$. Flows are stronger in this case so that this small discrepancy may arise from residual dissipation. We could also think of incorporating the angle between the drops' center axis and horizontal: Projecting the momentum on the vertical yields $U = U^*\varepsilon^3/(1 + \varepsilon^3)(1 + \varepsilon)$, a function that cannot be distinguished from Eq. (3) in Fig. 1(f).

Our findings on departing droplets might be useful to understand phenomena where water condensing on textured surfaces leaves the substrate after contact [7,10,12]. Then, a large proportion of coalescences concerns neighboring droplets with different sizes (owing to the random distribution of nuclei), for which a model of asymmetric merging is relevant. For future work, it would be of great interest to adapt our model to jumping microdrops, and discuss whether adhesion can limit the departing velocity of tiny droplets [10,12]. Likewise, spore discharge in ballistospore mushrooms

involves a drop-solid interaction [21–24]. In this case also, the ejection velocity is smaller than predicted by energy conservation. This might be questioned with our device by looking at the coalescence and takeoff of a drop contacting a hydrophilic bead.

We thank the Japanese Society for Promotion of Science that made possible this collaboration with a Summer Program fellowship. We thank the Direction Générale de l'Armement (DGA) for contributing to the financial support, Rose-Marie Sauvage and Thierry Midavaine for their constant interest, and Thales for cofunding this project. The photolithography masks were made using the University of Tokyo VLSI Design and Education Center (VDEC)'s 8 in. EB writer F5112+VD01 donated by ADVANTEST Corporation. This work was partially supported by JSPS KAKENHI Grant No. 25000010.

-
- [1] R. Blossey, Self-cleaning surfaces—virtual realities, *Nat. Mater.* **2**, 301 (2003).
 - [2] Y.-T. Cheng and D. E. Rodak, Is the lotus leaf superhydrophobic? *Appl. Phys. Lett.* **86**, 144101 (2005).
 - [3] Y.-T. Cheng, D. E. Rodak, A. Angelopoulos, and T. Gacek, Microscopic observations of condensation of water on lotus leaves, *Appl. Phys. Lett.* **87**, 194112 (2005).
 - [4] K. A. Wier and T. J. McCarthy, Condensation on ultrahydrophobic surfaces and its effect on droplet mobility: Ultrahydrophobic surfaces are not always water repellent, *Langmuir* **22**, 2433 (2006).
 - [5] C.-H. Chen, Q. Cai, C. Tsai, C.-L. Chen, G. Xiong, Y. Yu, and Z. Ren, Dropwise condensation on superhydrophobic surfaces with two-tier roughness, *Appl. Phys. Lett.* **90**, 173108 (2007).
 - [6] C. Dorrer and J. Ruehe, Wetting of silicon nanograss: From superhydrophilic to superhydrophobic surfaces, *Adv. Mater.* **20**, 159 (2008).
 - [7] J. B. Boreyko and C.-H. Chen, Self-Propelled Dropwise Condensate on Superhydrophobic Surfaces, *Phys. Rev. Lett.* **103**, 184501 (2009).
 - [8] K. Rykaczewski, W. A. Osborn, J. Chinn, M. L. Walker, J. H. J. Scott, W. Jones, C. Hao, S. Yao, and Z. Wang, How nanorough is rough enough to make a surface superhydrophobic during water condensation? *Soft Matter* **8**, 8786 (2012).
 - [9] R. Enright, N. Miljkovic, A. Al-Obeidi, C. V. Thompson, and E. N. Wang, Condensation on superhydrophobic surfaces: The role of local energy barriers and structure length scale, *Langmuir* **28**, 14424 (2012).
 - [10] J. Liu, H. Guo, B. Zhang, S. Qiao, M. Shao, X. Zhang, X.-Q. Feng, Q. Li, Y. Song, L. Jiang, and J. Wang, Guided self-propelled leaping of droplets on a micro-anisotropic superhydrophobic surface, *Angew. Chem., Int. Ed.* **55**, 4265 (2016).
 - [11] H. Cha, C. Xu, J. Sotelo, J. M. Chun, Y. Yokoyama, R. Enright, and N. Miljkovic, Coalescence-induced nanodroplet jumping, *Phys. Rev. Fluids* **1**, 064102 (2016).
 - [12] T. Mouterde, G. Lehoucq, S. Xavier, A. Checco, C. T. Black, A. Rahman, T. Midavaine, C. Clanet, and D. Quéré, Antifogging abilities of model nanotextures, *Nat. Mater.* **16**, 658 (2017).
 - [13] F. Liu, G. Ghigliotti, J. J. Feng, and C.-H. Chen, Self-propelled jumping upon drop coalescence on Leidenfrost surfaces, *J. Fluid Mech.* **752**, 22 (2014).
 - [14] F. Liu, G. Ghigliotti, J. J. Feng, and C.-H. Chen, Numerical simulations of self-propelled jumping upon drop coalescence on non-wetting surfaces, *J. Fluid Mech.* **752**, 39 (2014).
 - [15] C. Lv, P. Hao, Z. Yao, Y. Song, X. Zhang, and F. He, Condensation and jumping relay of droplets on lotus leaf, *Appl. Phys. Lett.* **103**, 021601 (2013).
 - [16] F.-C. Wang, F. Yang, and Y.-P. Zhao, Size effect on the coalescence-induced self-propelled droplet, *Appl. Phys. Lett.* **98**, 053112 (2011).
 - [17] R. Enright, N. Miljkovic, J. Sprittles, K. Nolan, R. Mitchell, and E. N. Wang, How coalescing droplets jump, *ACS Nano* **8**, 10352 (2014).
 - [18] T.-V. Nguyen, B.-K. Nguyen, H. Takahashi, K. Matsumoto, and I. Shimoyama, High-sensitivity triaxial tactile sensor with elastic microstructures pressing on piezoresistive cantilevers, *Sens. Actuators, A* **215**, 167 (2014).

HOW MERGING DROPLETS JUMP OFF A . . .

- [19] M. Gel and I. Shimoyama, Force sensing submicrometer thick cantilevers with ultra-thin piezoresistors by rapid thermal diffusion, *J. Micromech. Microeng.* **14**, 423 (2004).
- [20] M.-K. Kim, H. Cha, P. Birbarah, S. Chavan, C. Zhong, Y. Xu, and N. Miljkovic, Enhanced jumping-droplet departure, *Langmuir* **31**, 13452 (2015).
- [21] A. H. R. Buller, *Researches on Fungi*, Vol. 1 (Longmans, Green, and Co., London, 1909).
- [22] J. Turner and J. Webster, Mass and momentum transfer on the small scale: How do mushrooms shed their spores? *Chem. Eng. Sci.* **46**, 1145 (1991).
- [23] A. Pringle, S. N. Patek, M. Fischer, J. Stolze, and N. P. Money, The captured launch of a ballistospore, *Mycologia* **97**, 866 (2005).
- [24] X. Noblin, S. Yang, and J. Dumais, Surface tension propulsion of fungal spores, *J. Exp. Biol.* **212**, 2835 (2009).